Journal of Alloys and Compounds 511 (2012) 95–100

Contents lists available at SciVerse ScienceDirect

Journal of Alloys and Compounds

journal homepage: www.elsevier.com/locate/jallcom

Modification of the hydrogenation properties of $LaNi_5$ upon Ni substitution by Rh, Ir, Pt or Au

J. Prigent[a,b], J.-M. Joubert[a,*], M. Gupta[b]

[a] Chimie Métallurgique des Terres Rares, Institut de Chimie et des Matériaux Paris-Est, CNRS, Université Paris-Est, 2-8 rue H. Dunant, 94320 Thiais Cedex, France
[b] Laboratoire de Thermodynamique et Physico-Chimie des Hydrures et Oxydes, Université Paris-Sud Orsay, Bât 410, 91405 Orsay, France

ARTICLE INFO

Article history:
Received 27 July 2011
Received in revised form 29 August 2011
Accepted 31 August 2011
Available online 10 September 2011

Keywords:
Hydrogen absorbing materials
Intermetallics
Metal hydrides
Gas–solid reactions
Thermodynamic properties
Computer simulations

ABSTRACT

The hydrogenation properties of the $LaNi_{5-x}M_x$ (M = Rh, Ir, Au) compounds have been studied. The Ni substitution has several consequences: pressure plateau splitting and increase of plateau pressure. This latter observation disagrees with the general rule that a cell volume increase of the alloy should result in a plateau pressure lowering. In order to elucidate the origin of this anomalous behaviour, DFT calculations have been performed on both $LaNi_{5-x}Rh_x$ and $LaNi_{5-x}Pt_x$ intermetallic compounds, which, according to the present and previous experimental work, present a similar anomaly. We discuss our results in light of the models proposed in the literature. We conclude that, in the case of a Ni substitution by 4*d* or 5*d* elements, the size effect alone fails in predicting the hydrogen absorption properties while the rule of reverse stability is obeyed.

1. Introduction

$LaNi_5$ intermetallic compound (IMC) is well known for its ability to store hydrogen reversibly at pressure and temperature close to ambient conditions [1]. In this respect, it may serve as a reference compound to understand the physical and chemical phenomena influencing the hydrogen sorption properties. The effects of lanthanum and nickel substitution by many different elements on the thermodynamic properties, the hydrogen storage capacity or the ageing behaviour during hydrogen cycling have been studied in detail. Nevertheless, there is no clear and universal law to predict the influence of a substituting element on the stability of the hydride. In this paper, we have studied for the first time the hydrogen absorption thermodynamic properties of several $LaNi_{5-x}M_x$ compounds (M = Rh, Ir, Au) using the Sieverts method. Since no experimental data on the crystal structure of the hydrides of the substituted compounds with M = Rh, Ir, Au are yet available, the calculations of the enthalpies of formation were performed on the hydrides of the $LaNi_{5-x}Pt_x$ parent compounds presenting similar anomalous behaviour in the isotherms and for which detailed neutron scattering data on the deuterides have been analyzed in previous work by Joubert et al. [2]. The results are compared to existing empirical models in order to discuss the chemical and physical role of the substituting elements on the hydrogen sorption properties.

2. Results from previous works

A trend has been observed between the cell volume of the IMC and the logarithm of the plateau pressure of their hydrides: in $LaNi_5$ substituted compounds (but also for most hydride forming intermetallic compounds), any increase of the cell volume due to substitution is accompanied by a decrease of the hydrogen absorption plateau pressure, and thus a stabilization of the hydride (e.g., for substitution by Sn [3], Al [4], Mn [5], Co [6] or Cu [7]). This could suggest a simple geometrical model linking the size of the insertion sites and the ability of hydrogen to be stored in it. Yet, two exceptions to this model have been found: the substitution of nickel by palladium [8,9] or platinum [2] increases both the cell volume and the plateau pressure, leading to a destabilization of the substituted hydrides. These exceptions led us to extend the study of the $LaNi_5$ substituted compounds to other 4*d* and 5*d* substituting elements.

As detailed in our previous study [10] on the determination of the ternary phase diagrams of these systems, the $LaNi_{5-x}M_x$ IMCs (M = Rh, Ir, Au) have been synthesized using materials of high purity (>99.9%), melted in an arc furnace and annealed at 1273 K during 7 days under vacuum. The IMCs have been characterized by X-ray diffraction (XRD) using the Rietveld method and electron probe micro-analysis (EPMA). The compounds are all single-phase and crystallize with the $CaCu_5$ structure type ($P6/mmm$ space group).

* Corresponding author. Tel.: +33 1 49 78 12 11; fax: +33 1 49 78 12 03.
E-mail address: jean-marc.joubert@icmpe.cnrs.fr (J.-M. Joubert).

0925-8388/$ – see front matter © 2011 Elsevier B.V. All rights reserved.
doi:10.1016/j.jallcom.2011.08.094

Table 1
Characterization of the metallic samples. Lattice parameters are from XRD, compositions are from EPMA.

Nominal composition	Analysed composition	Cell parameters (Å)	Occupancy (at./site)	
			2*c* site	3*g* site
$LaNi_{4.5}Rh_{0.5}$	$La_{0.99(2)}Ni_{4.48(3)}Rh_{0.529(9)}$	$a = 5.0523(2)$ $c = 4.0017(2)$	0.16(2)	0.37(2)
$LaNi_4Rh$	$La_{0.990(5)}Ni_{4.006(9)}Rh_{1.004(5)}$	$a = 5.0901(1)$ $c = 4.0165(2)$	0.16(2)	0.84(2)
$LaNi_3Rh_2$	$La_{0.991(4)}Ni_{2.992(9)}Rh_{2.017(6)}$	$a = 5.1663(2)$ $c = 4.0491(2)$	0.13(3)	1.87(3)
$LaNi_2Rh_3$	$La_{0.99(1)}Ni_{2.01(1)}Rh_{3.00(9)}$	$a = 5.2298(2)$ $c = 4.0988(2)$	0.59(2)	2.41(2)
$LaNi_{4.5}Ir_{0.5}$	$La_{1.01(2)}Ni_{4.51(2)}Ir_{0.479(8)}$	$a = 5.0574(1)$ $c = 4.0044(1)$	0.041(3)	0.541(3)
$LaNi_{4.5}Au_{0.5}$	$La_{0.990(6)}Ni_{4.521(7)}Au_{0.489(3)}$	$a = 5.0810(1)$ $c = 4.0323(1)$	0.058(5)	0.442(5)
$LaNi_{4.35}Au_{0.65}$	$La_{0.989(5)}Ni_{4.373(5)}Au_{0.638(2)}$	$a = 5.1007(1)$ $c = 4.0467(1)$	−0.024(6)	0.664(6)
$LaNi_{4.2}Au_{0.8}$	$La_{0.980(5)}Ni_{4.241(5)}Au_{0.779(3)}$	$a = 5.1174(1)$ $c = 4.0624(1)$	0.051(7)	0.749(7)
$LaNi_4Au$	$La_{0.993(8)}Ni_{4.01(1)}Au_{0.993(8)}$	$a = 5.1443(1)$ $c = 4.0829(1)$	0.024(9)	0.976(9)

EPMA and XRD results are shown in Table 1. Among the two possible Ni substitution sites (2*c* and 3*g*), a clear preference of the substituting element for site 3*g* has been observed and discussed in detail previously [10]. This preference is frequently observed when substituting nickel by larger atoms (e.g., Pt[2], Sn[3] or Al[4]).

As shown by Joubert et al. [2], two hydrides can be observed in the $LaNi_{5-x}Pt_x$–H system: the β-hydride $LaNi_{4.75}Pt_{0.25}D_{5.23}$ crystallizes in the *P*6*mm* space group, as $LaNi_5H_6$[11]; the γ-hydride $LaNi_{4.25}Pt_{0.75}D_{2.61}$ crystallizes in the orthorhombic *Ibam* space group. The same structures are observed in the case of the γ-$LaNi_4PdH_3$ and β-$LaNi_{4.5}Pd_{0.5}H_5$ deuterides and have been previously studied using *ab initio* calculations [9].

3. Experimental and computational details

The hydrogen sorption properties of the compounds $LaNi_{5-x}Rh_x$ ($x = 0.5$; 1; 2; 3) have been studied. Iridium, like rhodium, has also a large solubility in $LaNi_5$, up to $LaNi_{2.5}Ir_{2.5}$ [12] but, due to experimental pressure limitations, we have only studied the compound $LaNi_{4.5}Ir_{0.5}$. Gold can substitute nickel up to $LaNi_{3.4}Au_{1.6}$, so the compound $LaNi_{5-x}Au_x$ ($x = 0.5$; 0.65; 0.8 and 1) have been investigated. The pressure-composition-isotherm (PCI) curves have been measured at 298 K with a Sievert apparatus. Before the measurements, the samples were activated by five cycles of hydrogenation in order to obtain stable and reproducible PCI curves.

The *ab initio* calculations have been performed within the pseudo-potential method based on all-electron projector augmented wave (PAW) potentials for the elemental constituents. The exchange and correlation terms are described using the generalized gradient approximation (GGA) of Perdew and Wang [13,14]. The calculations have been performed with the Vienna *ab initio* simulation package (VASP) [15,16]. The internal atomic coordinates and the lattice constants were fully relaxed. A dense grid of *k*-points in the irreducible wedges of the Brillouin zones of the different crystals insured a convergence of 10^{-6} eV/unit cell for the electronic energies, and the forces on the atoms after relaxation were smaller than 10^{-3} eV Å^{-1}. The enthalpies of formation of the intermetallic compounds and their corresponding hydrides were calculated using the total energies of the elemental solids, IMCs, hydrides and H_2 molecule obtained with the VASP code.

Only ordered compounds can be calculated, it is therefore necessary to use models approximating the real crystal structure and to adapt the symmetry operations accordingly (*i.e.* the space group is not always conserved). Platinum is only present on site 3*g* up to $x = 3$. In the $LaNi_4Pt$ model, the platinum atom replaces the nickel atom on one of the three equivalent positions (1/2 1/2 1/2). In the $LaNi_{4.5}Pt_{0.5}$ model, the $CaCu_5$-type cell is doubled along the *c* axis, making possible the replacement of one half of the Ni atom at this position.

Rhodium replaces nickel on both sites 2*c* and 3*g* and different structural models need to be compared. $LaNi_4Rh$ is built with a substitution on site 3*g* using the same model as for $LaNi_4Pt$. For $LaNi_3Rh_2$, two models are considered. In the "$LaNi_3Rh_2$ 3*g*" model, Rh is placed at (1/2 0 1/2) and (0 1/2 1/2). In the "$LaNi_3Rh_2$ 2*c*" model, site 2*c* is completely occupied by Rh. The compound $LaNi_2Rh_3$ is modelled by a complete replacement of nickel in site 3*g* by rhodium.

Starting from the experimental structural parameters, the volume and the *c*/*a* ratio have been calculated by minimization of the total energy for the different configurations used.

Concerning the calculation of the platinum substituted hydrides, we chose the composition $LaNi_4PtH_3$ and $LaNi_{4.5}Pt_{0.5}H_5$ as models of the γ and β hydrides. The distribution of the hydrogen atoms in the structure is based on the models previously established for the palladium substituted compounds [9]. This approximation is justified by a strong similarity of the crystallographic structures observed experimentally between the platinum and the palladium substituted deuterides [2,9]. The cell parameters are calculated by minimization of the total energy, starting from the experimental parameters measured by Joubert et al. [2].

4. Results

4.1. Hydrogenation properties

Fig. 1 shows the PCI curves of the compounds $LaNi_{5-x}Rh_x$. For $0 < x < 2$, we observed a single plateau. As a function of Rh content, the capacity slightly decreases and the plateau pressure regularly increases. A significant hysteresis is observed. The PCI curve of $LaNi_2Rh_3$ is somewhat different from those observed at lower Rh content. A wide solubility branch is observed before reaching a very short pressure plateau and hysteresis has disappeared

Fig. 2 shows the PCI curve of the compound $LaNi_{4.5}Ir_{0.5}$. The hydrogenation capacity is half to that of $LaNi_5$ and the plateau

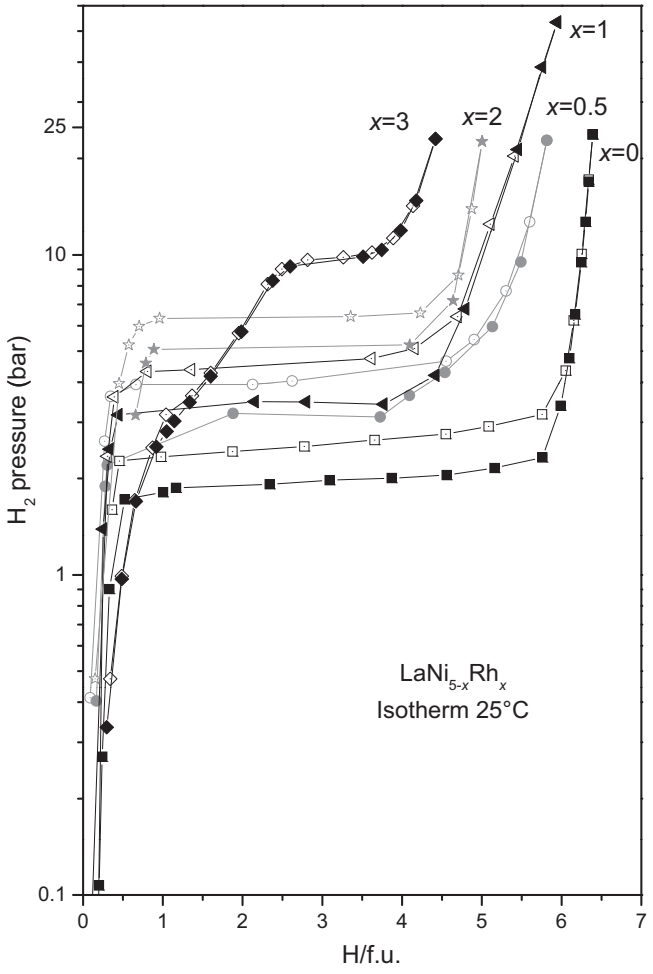

Fig. 1. hydrogen PCI curves of the $LaNi_{5-x}Rh_x$ compounds ($x = 0.5$; 1; 2; 3) at 25 °C. $LaNi_5$ ($x = 0$) is shown for comparison.

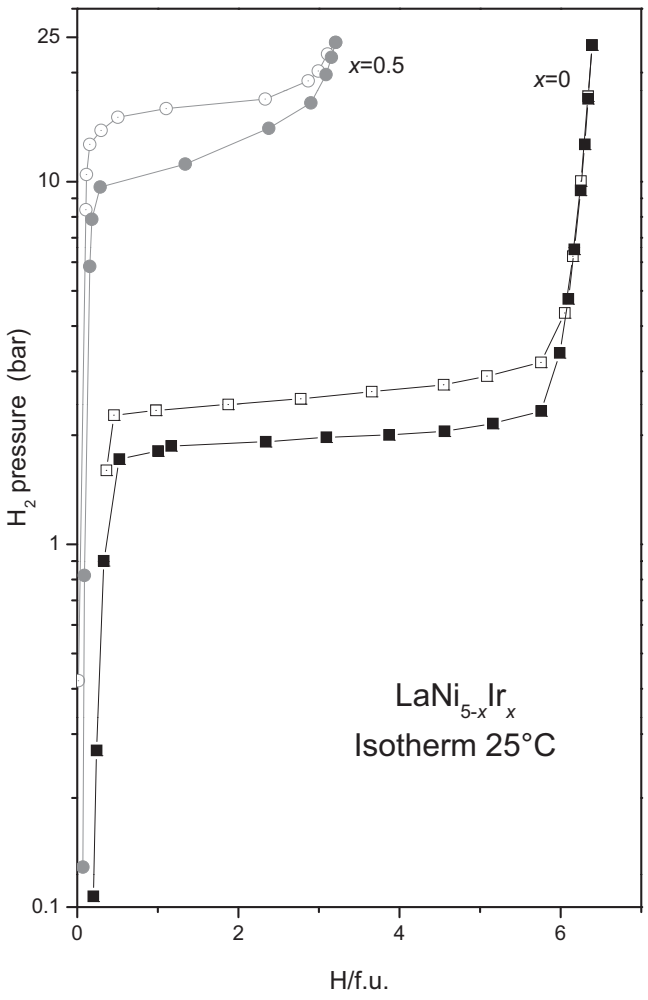

Fig. 2. hydrogen PCI curves of the $LaNi_{4.5}Ir_{0.5}$ compounds at 25 °C. $LaNi_5$ ($x = 0$) is shown for comparison.

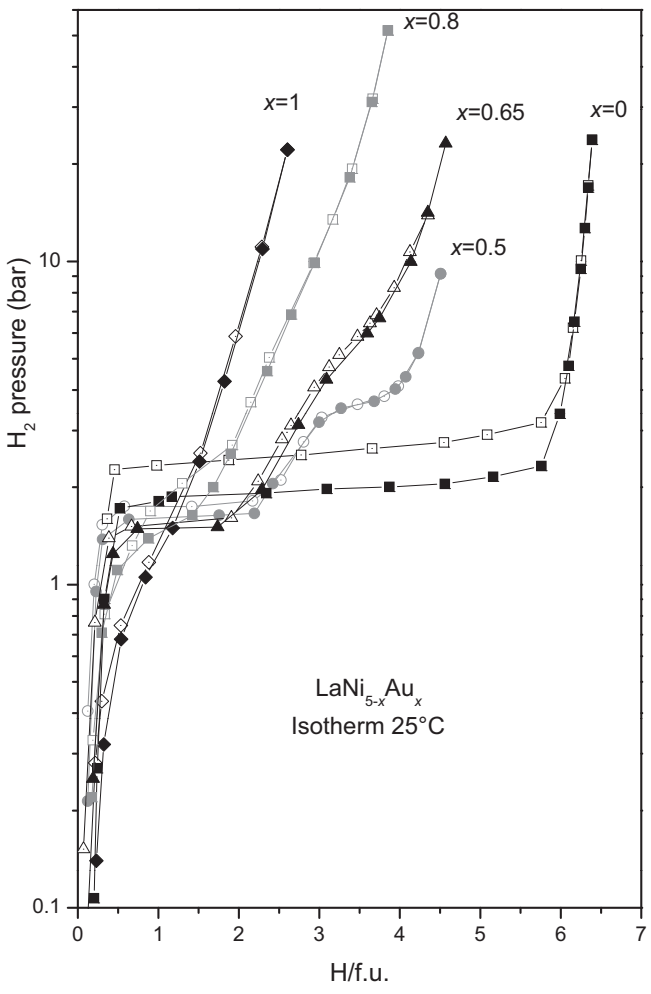

Fig. 3. hydrogen PCI curves of the $LaNi_{5-x}Au_x$ compounds ($x = 0.5$; 0.65; 0.8; 1) at 25 °C. $LaNi_5$ ($x = 0$) is shown for comparison.

pressure is much higher. The absorption plateau is well defined but the desorption plateau has a significant slope.

The PCI curves of the compounds $LaNi_{5-x}Au_x$ are shown Fig. 3. The compound $LaNi_{4.5}Au_{0.5}$ shows two pressure plateaus. The first one is observed between 0.3 H/f.u. and 2 H/f.u. at a lower pressure than that of $LaNi_5$. The second plateau is observed between 3 H/f.u. and 4 H/f.u. at a higher pressure than that of $LaNi_5$. The compound $LaNi_{4.35}Au_{0.65}$ shows also a first plateau with a extent similar to that found for $LaNi_{4.5}Au_{0.5}$ but is observed at a lower pressure. The second plateau shrinks so that we only observed an inflexion in the PCI curve at higher pressure than the second plateau of $LaNi_{4.5}Au_{0.5}$. In the case of the compound $LaNi_{4.2}Au_{0.8}$, the second plateau has disappeared and the first plateau is strongly leaned. Yet, we can observe a hysteresis phenomenon between absorption and desorption, which may be an indication that a phase transition is still present. The compound $LaNi_4Au$ does not show plateau anymore.

4.2. Ab initio calculations

As shown in Table 2, the calculated lattice parameters of the IMCs agree within a few percent with the experimental values. Fig. 4 compares the total DOS for the IMCs substituted with rhodium.

The enthalpies of formation of the IMCs have been calculated according to the following reaction:

$$La + (5-x)Ni + xM \rightarrow LaNi_{5-x}M_x \quad \text{with} \quad M = \text{RhorPt} \qquad (1)$$

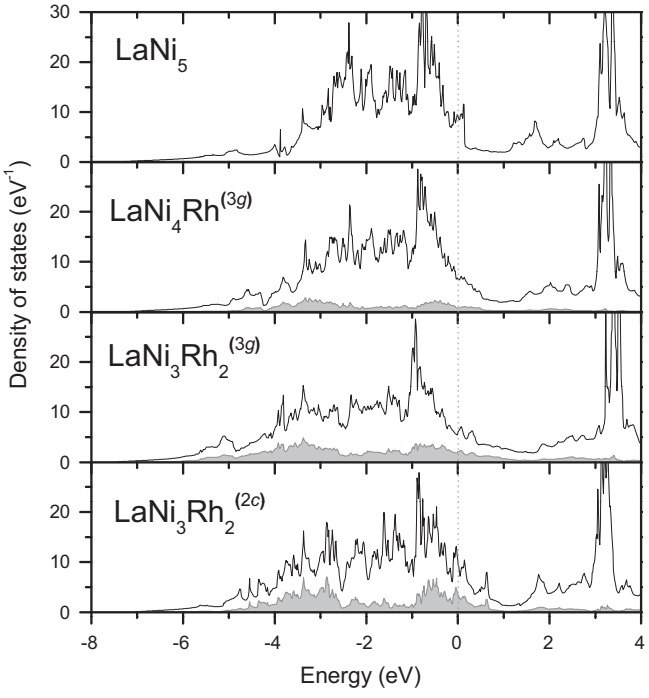

Fig. 4. Total density of states (black line) and contribution of the rhodium atoms (in grey) of the IMCs. The Fermi level is chosen as the origin of the energy.

Table 2
Results of the *ab initio* calculations of the IMC compounds. For the different compositions and models tested, the cell parameters are compared to the experimental ones.

IMC	Ni substitution on 2*c* site	Ni substitution on 3*g* site	Calculated *a* (Å) *c* (Å) *V* (Å^3)	Experimental *a* (Å) *c* (Å) *V* (Å^3)	Ref.	ΔH_f (kJ (mol f.u.)$^{-1}$)
$LaNi_5$	0	0	4.8627 3.8578 78.9997	5.020 3.980 86.860	[1]	−166 exp. [23] −170 calc. [9] −168 calc. [24]
$LaNi_4Rh$	0	1	4.9519 3.9461 83.7998	5.0901 4.0165 90.122	[10]	−243.6
$LaNi_3Rh_2$ 2*c*	2	0	4.9802 4.0940 87.9368 *c*/*a* = 0.8221	5.1663 4.0491 93.594 *c*/*a* = 0.7838	[10]	−256.7
$LaNi_3Rh_2$ 3*g*	0	2	5.0680 3.9495 87.851 *c*/*a* = 0.7793			−300.9
$LaNi_2Rh_3$ 3*g*	0	3	5.1356 3.9924 91.1891	5.2298 4.0988 97.086	[10]	−358.4
$LaNi_{4.5}Pt_{0.5}$	0	0.5[a]	5.0734 4.0174 89.5517	5.064 4.010 89.056	[2]	−219
$LaNi_4Pt$	0	1	5.1260 4.0517 92.1988	5.113 4.039 91.444	[2]	−273

[a] The cell used for the calculation is a double $CaCu_5$-type cell along the *c* axis, one cell is substituted with a platinum atom on the central 3*g* site, the other is without substitution.

Thus,

$$\Delta H_f^{LaNi_{5-x}M_x} = E_{tot}^{LaNi_{5-x}M_x} - (E_{tot}^{La} + (5-x)E_{tot}^{Ni} + xE_{tot}^{M}) \quad (2)$$

Figs. 5 and 6 show the DOS diagrams of the γ-$LaNi_4PtH_3$ and β-$LaNi_{4.5}Pt_{0.5}H_5$ hydrides, respectively. Considering the total energies of the IMC, the hydride and the hydrogen molecule, it is possible to determine the enthalpy of formation of the hydride:

$$LaNi_{5-x}M_x + y/2H_2 \rightarrow LaNi_{5-x}M_xH_y \quad (3)$$

Thus,

$$\Delta H_f^{hydride} = E_{tot}^{hydride} - E_{tot}^{IMC} - \frac{y}{2}E_{tot}^{H_2} \quad (4)$$

The results of these calculations are summarized and compared with the IMC enthalpies of formation in Table 3.

5. Discussion

5.1. Hydrogen absorption in the $LaNi_{5-x}M_x$ system (M = Rh, Ir, Au)

The PCI curve of the compound $LaNi_2Rh_3$ shows a large shoulder at low hydrogen content indicating a large solubility of hydrogen before the formation of the hydride. However, no increase of the solid solution domain was noticed for $0 \le x \le 2$. The sudden change of PCI shape between $x = 2$ and $x = 3$ is difficult to explain.

The substitution by iridium has a really strong destabilizing effect on the hydride formation and the limit of our pressure

Table 3
Calculated enthalpies of formation of the $LaNi_{5-x}Pt_x$ IMC and hydrides. The experimental values [23] obtained for $LaNi_5$ and the hydride $LaNi_5H_6$ are also reported for comparison together with the results of calculations [9,24] on $LaNi_5$ and $LaNi_5H_7$.

IMC	ΔH_f^{IMC}	Hydride	$\Delta H_f^{hydride}$
$LaNi_5$ [23]	−166 kJ (mol f.u.)$^{-1}$	$LaNi_5H_6$ [23]	−30.5 kJ (mol H_2)$^{-1}$
$LaNi_5$ [9]	−170 kJ (mol f.u.)$^{-1}$	$LaNi_5H_7$ [9]	−40 kJ (mol H_2)$^{-1}$
$LaNi_5$ [24]	−168 kJ (mol f.u.)$^{-1}$	$LaNi_5H_7$ [24]	−38.2 kJ (mol H_2)$^{-1}$
$LaNi_{4.5}Pt_{0.5}$	−219 kJ (mol f.u.)$^{-1}$	$LaNi_{4.5}Pt_{0.5}H_5$	−28 kJ (mol H_2)$^{-1}$
$LaNi_4Pt$	−273 kJ (mol f.u.)$^{-1}$	$LaNi_4PtH_3$	−24.6 kJ (mol H_2)$^{-1}$

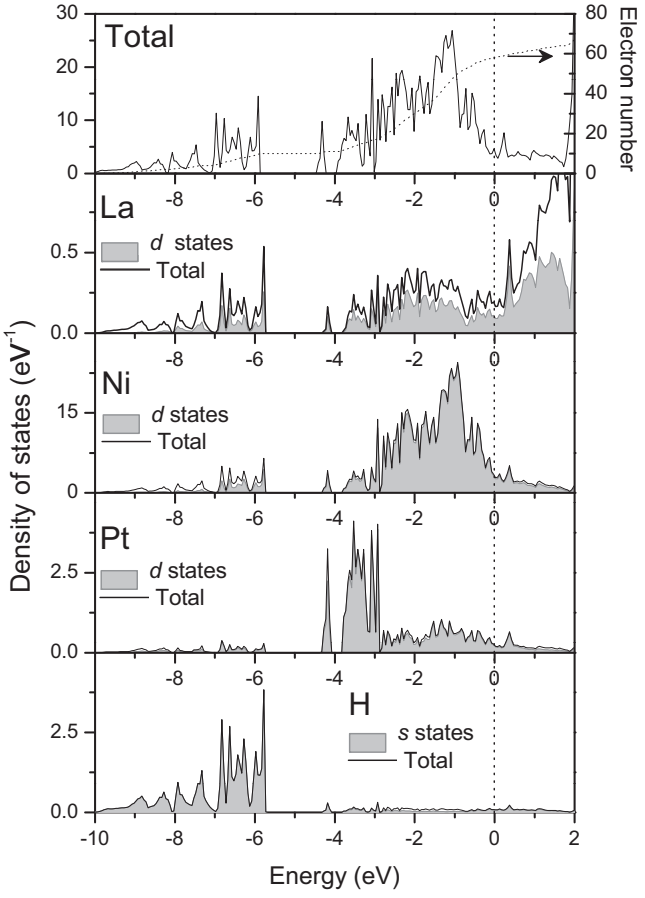

Fig. 5. Total and partial density of states of the hydride $LaNi_{4.5}Pt_{0.5}H_5$ (β phase). In the partial DOS, the contribution of the atom is drawn with a line. The contribution of the main orbital is represented in grey.

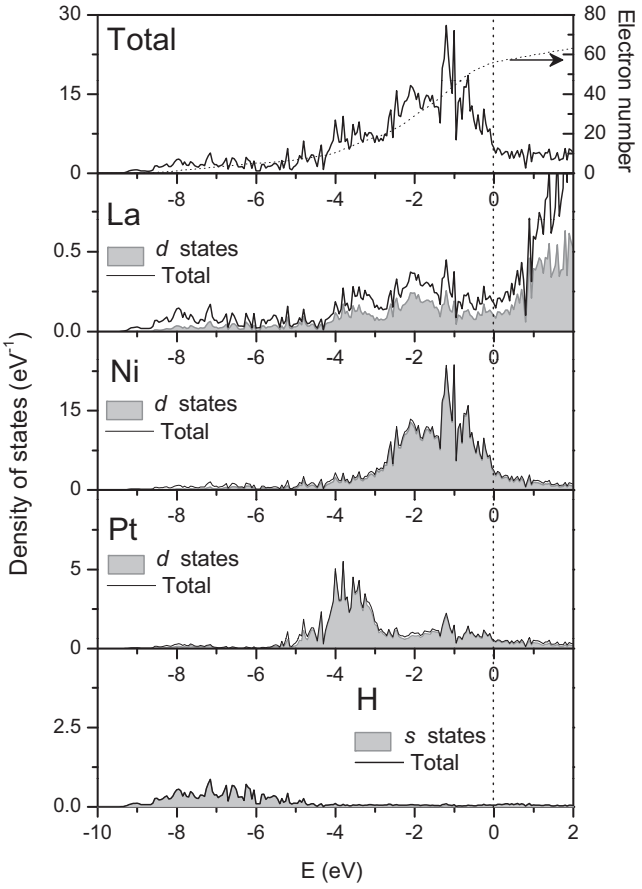

Fig. 6. Total and partial density of states of the hydride $LaNi_4PtH_3$ (γ phase). In the partial DOS, the contribution of the considered atom is drawn with a line. The contribution of the main orbital is represented in grey.

sensors is rapidly exceeded. It cannot be excluded that the $LaNi_{4.5}Ir_{0.5}$ compound presents a second plateau at higher pressures. A high pressure Sieverts apparatus would be needed to further explore the effects of iridium substitution above $x = 0.5$.

The gold substitution generates two absorption plateaus at low substitution rate. Increasing gold substitution, the capacity is strongly reduced and the plateaus disappear rapidly. This behaviour is similar to what is observed with palladium substitution [9]. The presence of two plateaus demonstrates that an intermediate hydride γ is formed between the solid solution α and the terminal hydride β. The two-phase domains γ – β and α – β disappear quickly as a function of *x*. The variation of the plateau pressures is different for the first and for the second plateau. The fact that the first plateau pressure decreases whereas the second one increases with *x* is remarkable.

5.2. Electronic structure

In Fig. 4, the total DOSs of the rhodium substituted compounds $LaNi_{5-x}Rh_x$ are plotted for $x = 0$; 1 and 2. In the reference IMC $LaNi_5$ ($x = 0$), the occupied states of the valence band are mainly composed of Ni-3*d* states hybridized with La-5*d* states, with a smaller contribution of the Ni and La *s* and *p* states. $LaNi_5$ is not a charge transfer compound [17] since the Ni-3*d* states, of total width 3.5 eV are not entirely filled. The broad empty La-5*d* states are mainly centred above the Fermi level while the peak of the DOS located at ≈3 eV above the Fermi level corresponds to the empty La-4*f* states. It is clear from Fig. 4 that the contribution of the Rh-4*d* states increases in width and intensity as the Rh concentration increases. The broadening of the DOS with increasing values of *x* is associated with the much larger spatial extension of the Rh-4*d* versus Ni-3*d* orbitals. Similar trend has been found in our previous work [9] on Pd substituted compounds $LaNi_{5-x}Pd_x$.

The total DOS of the hydrides $LaNi_{4.5}Pt_{0.5}H_5$ and $LaNi_4PtH_3$, plotted in the upper part of Figs. 5 and 6, present two main structures. Just under the Fermi level, down to −4.5 eV and −5.4 eV for $LaNi_{4.5}Pt_{0.5}H_5$ and $LaNi_4PtH_3$, respectively, we find the states due to the metal-metal interactions as in the corresponding IMC. These states are dominated by the Ni-3*d* bands and a small contribution of the Pt-4*d* bands. At low energy, a structure due to the metal–hydrogen bonding is observed. As the hydrogen content increases, these bonding states split to lower energies from the main part of the transition metal *d* bands and their intensity grows. In its low-energy part (<−8 eV), the H-1*s* electrons interact mainly with the *s*–*p* electrons of the transition elements whereas, in the high energy part of the structure (above −8 eV), they interact with the *d* electrons of the two transition elements. Due to the small platinum content, the interactions occur mainly between hydrogen and nickel. The DOS curves are very similar between hydrides substituted with platinum or palladium [9].

The calculated enthalpies of formation of the IMCs $LaNi_{5-x}M_x$ (M = Rh, Pt) reported in Table 2 are more negative when the substitution rate *x* increases. Thus rhodium and platinum have a stabilizing effect on the $CaCu_5$ structure. Although, to our knowledge, no experimental data on the formation enthalpies of these alloys are available in the literature, the compound $LaPt_5$ is known to be more stable than $LaNi_5$ since its experimental formation enthalpy (−461 kJ/f.u.) [18], is much more negative than that of $LaNi_5$ (−166 kJ/f.u.). The trend found in our calculated formation enthalpies of $LaNi_{5-x}Pt_x$ ($x = 0.5$, 1.0) indicates, in agreement with the experimental data, an increased stability of the platinum substituted alloys as *x* increases.

For the compound $LaNi_3Rh_2$, the calculations indicate that the substitution occurs preferentially at the site 3*g* rather than at the site 2*c* in agreement with the experimental results. Experimentally, however, site 2*c* is also partly occupied by Rh and we can suppose that the energy minimum could be observed between the two values calculated here. Moreover, Lundin et al. [17] demonstrated that the *c*/*a* ratio depends on the substitution rate on sites 3*g* and 2*c*. We can observe that the experimental *c*/*a* ratio is between the two theoretical ratios obtained in the calculations.

The enthalpies of formation of the hydrides of the Pt substituted compounds have been calculated, with $LaNi_5H_7$ hydride computed as a Ref. [9,24]. As shown in Table 3, they are less negative as a function of platinum content, a result that is in perfect agreement with the increase of the equilibrium plateau pressure observed experimentally [2].

5.3. Hydride stability

As explained in paragraph 2, the geometric criterion allows us to describe the pressure dependence for a large number of substitutions such as rare earths on La site, or Mn, Al, Co on Ni sites. As shown in Fig. 7 the plateau pressure logarithm decreases as a function of the cell volume following a unique linear law for these elements, while for substituting elements (such as Cu, Fe, Sn on Ni sites) another, but still decreasing, linear law is obeyed.

The PCI curves measured in the present work show that the substitutions by rhodium or iridium increase the plateau pressure. Thus, the exceptions previously observed for the Ni substitution by palladium [9] and platinum [2] can be extended in all these systems: the plateau pressure increases despite an increase of the cell volume due to substitution. The case of $LaNi_{5-x}Au_x$ compounds deserves additional comments. Due to its larger size, Au substitution provokes the largest cell volume increase per substituted atom.

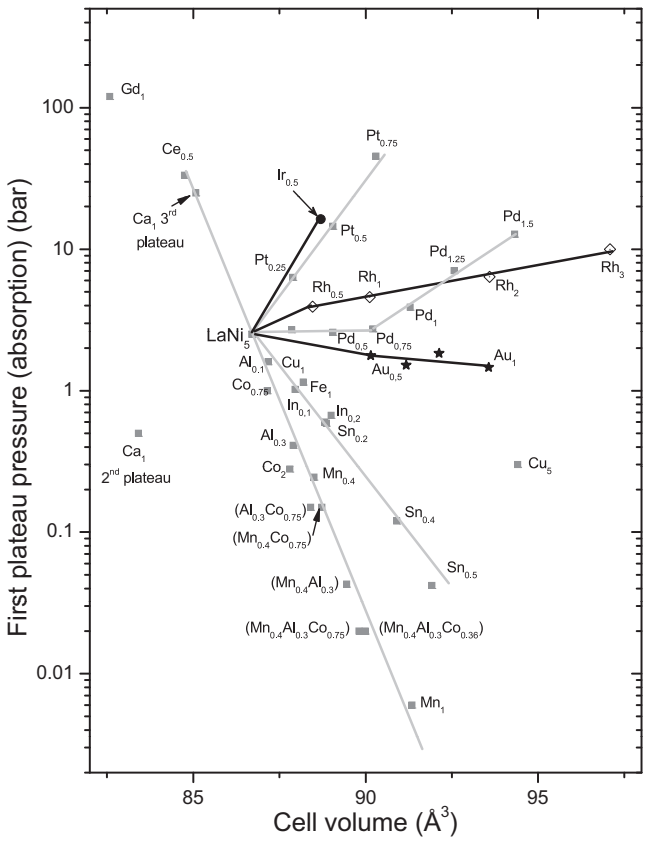

Fig. 7. Absorption first plateau pressure (otherwise indicated) at 25 °C as a function of the cell volume for $La_{1-y}R_yNi_{5-x}M_x$ compounds (R = Ca [25], Ce [26], Gd [27], M = Al, Co, Cu, Fe, Mn [26], Pd [9], In [28], Sn [3], Pt [2], Rh, Ir, Au, from present work).

It yields plateau splitting and the corresponding plateau pressures vary in an opposite way as a function of x.

It is clear that a geometric contribution to the plateau pressure variations is important as testifies the fact that the pressure–volume relationship is linear in most systems. Increase of the cell volume yields larger interstitial sites and correlated greater hydride solubility as has been shown also for Laves phase compounds [19].

However other contributions may in some cases counterbalance the pressure decrease induced by the cell volume increase caused by the substitution. As shown by our experimental results, such contribution seems to be particularly important for substitutions by 4*d* and 5*d* metals. More precisely, an increase of the slope of the straight line representing ln (P) as a function of V is always observed when changing a substituting element by another element below in the same column (see e.g. the straight lines defined by Co, Rh and Ir substitutions, that of Pd and Pt, and that of Cu and Au).

However, no direct correlation with the atomic number could be evidenced as shown, for example, by the case of tin which follows the same law as iron.

Another possible explanation for the differences between the elements could be the difference of binary hydride stability. The fact that platinum and rhodium form hydrides only in extreme pressure conditions [20,21] while nickel can be hydrogenated in softer conditions [22] could explain the destabilization of the hydrides when substituting these elements. However, the case of palladium which forms stable hydrides but the substitution of which destabilizes $LaNi_5$ hydrides contradicts this hypothesis.

Using *ab initio* calculations, we were able to calculate the enthalpies of formation of platinum and rhodium substituted IMC and that of $LaNi_4PtH_3$ and $LaNi_{4.5}Pt_{0.5}H_5$ hydrides. The substitution of Ni by these 4*d* and 5*d* atoms significantly stabilizes the IMC and the hydrides are less stable than $LaNi_5H_6$. These results are in accordance with the so-called rule of the reverse stability [8], which states that the more stable is the intermetallic compound, the less stable should be the hydride.

6. Conclusions

The hydrogen sorption properties of $LaNi_{5-x}M_x$ (M = Rh, Ir, Au) were studied. The substitution of nickel by these 4*d* and 5*d* elements increases the cell volume of the intermetallic compound but leads to a destabilization of the hydrides. This phenomenon contradicts the general behaviour observed in the case of a substitution of Ni by 3*d* and *p* elements but is similar to what is observed when nickel is substituted by palladium or platinum. *Ab initio* calculations were done on rhodium and platinum substituted intermetallic compounds and platinum substituted hydrides. They prove that the substitution stabilizes the intermetallic compounds and destabilizes the hydrides under study.

The substitution by these elements induces two opposite effects: an increase of the cell volume of the IMC stabilizing the hydride and a stabilization of the intermetallic compound yielding a destabilization of the hydride according to the rule of reverse stability. It seems that in the case of Ni, the substitution by 4*d* and 5*d* elements, the latter effect prevails.

References

[1] J.H.N. Van Vucht, F.A. Kuijpers, H.C.A.M. Bruning, Philips Res. Rep. 25 (1970) 133–146.
[2] J.-M. Joubert, J. Charton, A. Percheron-Guegan, J. Solid State Chem. 173 (2003) 379–386.
[3] J.-M. Joubert, M. Latroche, R. Cerný, R.C. Bowman Jr., A. Percheron-Guégan, K. Yvon, J. Alloys Compd. 293–295 (1999) 124–129.
[4] J.-C. Achard, A.-J. Dianoux, C. Lartigue, A. Percheron-Guégan, F. Tasset, in: G.J. McCarthy, H.B. Silber, J.J. Rhyne (Eds.), The Rare Earths in Modern Science and Technology, Plenum, New York, 1982, pp. 481–486.
[5] C. Lartigue, A. Percheron-Guégan, J.-C. Achard, J. Less Common Met. 75 (1980) 23–29.
[6] A.N. Pirogov, A.S. Yermolenko, V.N. Dvinyaminov, V.V. Chuyev, V.V. Kelarev, Phys. Met. Metall. 49 (3) (1980) 120–124.
[7] M. Latroche, J.M. Joubert, A. Percheron-Guégan, P.H.L. Notten, J. Solid State Chem. 146 (1999) 313–321.
[8] H.H. Van-Mal, K.H.J. Buschow, A.R. Miedema, J. Less Common Met. 35 (1974) 65–76.
[9] J. Prigent, J.-M. Joubert, M. Gupta, J. Solid State Chem. 184 (2011) 123–133.
[10] J. Prigent, J.-M. Joubert, Intermetallics 19 (2011) 295–301.
[11] C. Lartigue, A.L. Bail, A. Percheron-Guégan, J. Less Common Met. 129 (1987) 65–76.
[12] G.K. Malani, R.C. Mohanty, A. Raman, Z. Metallkd. 83 (5) (1992) 342–348.
[13] J.P. Perdew, Phys. Rev. B: Condens. Matter Mater. Phys. 33 (1986) 8822–8824.
[14] J.P. Perdew, Y. Wang, Phys. Rev. B: Condens. Matter Mater. Phys. 33 (1986) 8800–8802.
[15] G. Kresse, J. Hafner, J. Phys. Condens. Matter 6 (1994) 8245–8257.
[16] G. Kresse, J. Furthmuller, Comput. Mater. Sci. 6 (1996) 15–50.
[17] C.E. Lundin, F.E. Lynch, C.B. Magee, J. Less Common Met. 56 (1977) 19–37.
[18] S. Reimann, H.-J. Schaller, J. Alloys Compd. 419 (2006) 133–139.
[19] M. Boulghallat, N. Gerard, O. Canet, A. Percheron-Guegan, Z. Phys. chem. 179 (1993) 199–209.
[20] V.E. Antonov, I.T. Belash, V.Y. Malyshev, E.G. Ponyatovsky, Int. J. Hydrogen Energy 11 (1986) 193–197.
[21] O. Degtyareva, J.E. Proctor, C.L. Guillaume, E. Gregoryanz, M. Hanfland, Solid State Commun. 149 (2009) 1583–1586.
[22] B. Baranowski, K. Bochenska, Z. Phys Chem. N.F. 45 (1965) 140–152.
[23] C. Colinet, A. Pasturel, A. Percheron-Guégan, J.C. Achard, J. Less Common Met. 134 (1987) 109–122.
[24] J.F. Herbst, L.G. Hector Jr., J. Alloys Compd. 446–447 (2007) 188–194.
[25] G.D. Sandrock, J.J. Murray, M.L. Post, J.B. Taylor, Mater. Res. Bull. 17 (1982) 887–894.
[26] J.-M. Joubert, M. Latroche, R. Cerný, A. Percheron-Guégan, K. Yvon, J. Alloys Compd. 330–332 (2002) 208–214.
[27] J.L. Anderson, T.C. Wallace, A.L. Bowman, C.L. Radosevich, M.L. Courtney, in: Rep. LA-5320-MS, Los Alamos Science Laboratory, 1973.
[28] V.A. Yartys, R.V. Denys, B.C. Hauback, H. Fjellvag, I.I. Bulyk, A.B. Riabov, Y.M. Kalychak, J. Alloys Compd. 330–332 (2002) 132–140.